

Shear-Induced Reversibility of 2D Brownian Colloids

Somayeh Farhadi and Paulo E. Arratia

Department of Mechanical Engineering and Applied Mechanics,
University of Pennsylvania, Philadelphia, Pennsylvania 19104, USA

(Dated: August 26, 2016)

We experimentally investigate the dynamics of particle rearrangements for a 2D Brownian colloidal suspension under cyclic shear. We find that, even though the system is liquid-like and non-rigid ($\phi \leq 0.32$), a fraction of particles undergo reversible cycles, in the form of scattered particle clusters. Unlike jammed athermal systems, the reversible clusters are not stable and the particles transition between reversible and irreversible cycles. We demonstrate that the stability of reversibility depends both on ϕ and strain amplitude. We also identify plastic reversibility for our thermal system. However, as ϕ is decreased deep into liquid phase, the hysteresis in particle rearrangements becomes less prominent, and the dynamics is moved closer to equilibrium by thermal noise.

PACS numbers: 05.65.+b, 64.70.pv, 63.50.Lm

Colloids have been widely used as a model for disordered molecular and atomic systems such as soft and metallic glasses [1, 2], where particle positions can not easily be measured [3]. In particular, colloidal suspensions can be very useful in the study of particle-scale fluctuations associated with mesoscale rearrangements, which subsequently affect the material properties [1]. In general, particle fluctuations in colloidal suspensions are governed by two distinct mechanisms: Brownian (thermal) motion and externally driven deformations (e.g. shear). Recent numerical simulations suggest that an effective temperature exists for dense systems, which sets the energy scale of shear-induced fluctuations [4, 5]. Yet, with some notable exceptions [6, 7], very few experiments have directly measured thermal fluctuations of colloids in presence of shear. One of our goals in this study is to describe the collective effects of thermal and shear-induced fluctuations on the dynamics of particle rearrangements.

The phenomena related to thermal fluctuations in colloidal suspensions are sensitive to packing fraction, ϕ [8]. For instance, spontaneous rearrangements and equilibration due to thermal fluctuations are rare in jammed (dense) states. Hence, a highly packed system is relatively more distant from equilibrium compared to a dilute system [8]. As ϕ is lowered below the glass transition, even without external driving and given enough time, particles rearrange and diffuse, which subsequently moves the system towards an equilibrated state. One way to maintain a truly out of equilibrium state is to apply shear. This alternative framework allows us to study glass dynamics without encountering ageing phenomena, and is experimentally less challenging [9, 10]. As a result, there has been growing interest in experiments on glassy systems under shear.

Recently, the microstructure of an athermal colloidal suspension under cyclic shear was investigated [11–13]. The study showed that above yielding strain, the majority of particles rearranged stroboscopically, while below yielding, after a quick transient state, particle re-

arrangements were stroboscopically reversible[12]. Furthermore, close enough to yielding, a significant number of reversible particles underwent rearrangements which started and completely reversed within a given cycle, and had hysteresis. This regime was known as *plastic reversible*. In this study, we further investigate the existence of plastic reversible states, as thermal noise is added to the particle trajectories.

Particle rearrangements in colloidal suspensions are traditionally measured either by confocal microscopy or light scattering [1, 14–19]. In confocal microscopy, the time resolution of measurements is limited by scanning time. And for scattering, the trajectories of individual particles are not available, and instead, only the correlated motion of a large group of particles is probed. Here, by using a custom-made interfacial shearing apparatus ([11–13]), we shear and track nearly 2×10^4 Brownian particles adsorbed at an oil-water interface, and study the reversibility, as well as the onset of rearrangement, for each particle.

In this paper, we show that for a model 2D thermal colloidal suspension which is diluted to a liquid-like state, reversible particle clusters are still observed. However, unlike dense athermal systems, reversibility is not stable, and the particles transition between irreversible and reversible cycles. And the transition probabilities depend both on strain amplitude, γ_0 , and packing fraction, ϕ . We note that stroboscopic reversibility gives us useful information on the fabric of configurational energy landscape. In particular, it manifests the existence of energy metabasins which restrict the dynamics of the system. Our data shows that the dynamics within these metabasins is strongly affected by thermal noise. We also identify plastic reversibility, and by lowering ϕ , which in turn enhances thermal fluctuations, the number of plastic reversible particles decrease dramatically.

The schematics of our custom made setup is shown in Fig. 1. It consists of a 10 cm diameter Petri dish, and two external Helmholtz coils which are used to induce shear

force on a magnetized needle, which subsequently shears the colloidal matter. We have made a small apparatus (Fig. 1a,b), which holds two 1.8cm coverslip glasses. A spacer of width 15.9 mm is inserted between these coverslips. After placing the apparatus inside the Petri dish, we pour DI water, and then carefully add a thin oil layer (Decane 99+% from ACROS). The polar components of decane is removed by crossing the oil from aluminiumoxide powder (Acros Chemical, acidic activated, particle size 100-500 μm). The height of the water phase is such that the tips of the coverslips touch the interface, and hence, a meniscus is formed at the interface between two coverslips. We then carefully place the thin needle at the interface, between two coverslip walls. The needle is 4cm long, with diameter 0.15mm, and is cut from Phosphate-Coated carbon steel wire (from McMaster-Carr). The mass of the needle is low enough (4mg), such that the surface tension holds it at the interface. Prior to setup preparation, all of the parts are sonicated and rinsed with DI water, followed by a rinse with ethanol to avoid any aggregation inducing contaminations.

The colloidal particles used in this experiment are Sulfate Latex Beads, 8% w/v from invitrogen. These microspheres are charge-stabilized in DI water due to their surface sulphate treatment. Once they are placed at the interface, they form dipoles with a long-range and purely repulsive interaction force. Equal volumes of 1 μm and 1.2 μm particles are taken out of the bottle and mixed. We dilute 0.1mL of the mixture to 1mL with DI water, and add 0.5mL Isopropanol (Molecular Biology Grade, Fisher) for easy dispersion at the interface. The particle mixture is then slowly injected to the interface by a micropipet. More details on the preparation protocol is provided in references [11–13]. By injecting different volumes of particle suspension, we control the area fraction at the interface. In this study, we provide data for two area fractions: $\phi = 0.20$, and $\phi = 0.32$. The particle monolayer is imaged with a long-distance microscope (K2/SC Infinity Photo-Optical) and high-speed camera (Flare 4M180, IOIndustries). Within the recorded images (Fig. 1d), 1 μm particles approximately span 9 pixels, and the average particle spacing (σ) is 12.5(9.8) pixels for $\phi = 0.20(\phi = 0.32)$ system. The temperature is kept constant for all of the data.

The two external Helmholtz coils trap the needle at the interface, between two parallel walls. By adding an additional oscillatory current to one of the coils, we induce sinusoidal force on the needle. We then measure the displacement response of the needle, which provides strain measurements. The needle is driven with frequency $f = 0.1\text{Hz}$, and the data is taken at 40, 60, or 80 fps. Before each experiment, we apply 3 large amplitude cycles ($\gamma_0 = 1.0$), to avoid memory effects. The strain amplitudes of the data are varied within the interval $0.01 < \gamma_0 < 0.2$, and upto 60 cycles are recorded. A sample video of the experiment is provided in the Sup-

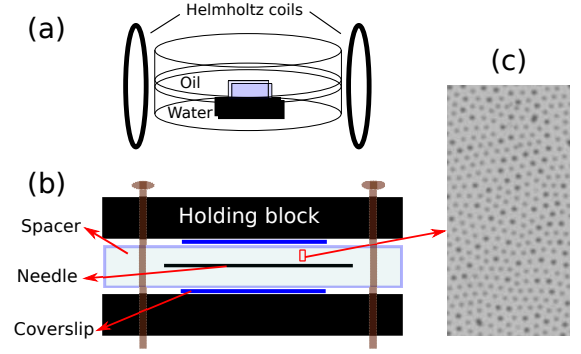


FIG. 1. a) Schematics of the shearing cell. b) Schematics of the spacer apparatus (top view). c) Mixture of 1 and 1.2 particles visualized under microscope. The area fraction is $\phi = 0.20$.

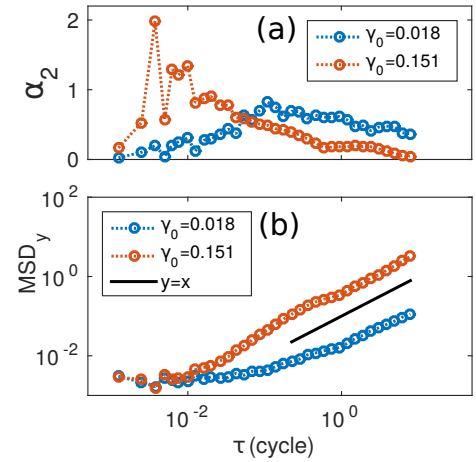


FIG. 2. a) Non-Gaussian measure, α_2 b) Mean square displacement of particles, measured for perpendicular to shear direction (The unit is σ^2). Here, $\phi = 0.32$.

plementary Materials. The images are then processed by *trackpy*, a python based particle tracking package[20]. For each data set, nearly 2×10^4 particles are identified and tracked.

The analysis of particle dynamics perpendicular to shear direction shows a liquid-like behaviour. One measure to describe the dynamics of glass forming liquids is the non-Gaussian parameter, $\alpha_2(\Delta t) = \frac{\langle \Delta x^4 \rangle}{3 \langle \Delta x^2 \rangle^2} - 1$. The peak of α_2 characterizes the time scale of cage rearrangements (or α -relaxations). The behaviour of $\alpha_2(\Delta t)$ has also shown to indicate the state of the system with respect to glass transition point [14, 17]. The shape of α_2 in Fig. 2a (plotted for $\phi = 0.32$ system) is consistent with a supercooled liquid. Also, the mean squared displacement curves (Fig. 2b) show diffusive behaviour at longer times, contrary to the expected sub-diffusive behaviour for jammed states[17]. We conclude (by induction) that the lower packing system, $\phi = 0.20$, is also liquid-like.

Using tracking data, we now quantify the stroboscopic

rearrangements of particles after completing each cycle. In order to do so, we use the quantity D_{min}^2 [21], defined as $D_{min}^2 = \Sigma(r'_i - \mathbf{E}r_i)^2$, which is a measure of nonaffinity of particle displacements. Here, r'_i and r_i are the positions of a group of particles in two different snapshots. For a given particle, the group is chosen as all of the particles centered within 2.5 diameter size distance. \mathbf{E} is the least squares fit, which transforms r_i to r'_i affinely: ($r'_i = \mathbf{E}r_i$). The spatial distribution of rearranging particles (of an arbitrary cycle) is shown for strain amplitudes $\gamma_0 = 0.017$ and $\gamma_0 = 0.158$, and for $\phi = 0.20$ system in Fig. 3a,b. The Red color demonstrates the rearranging region, whereas blue indicates reversible particles. Here, we take $D_{min}^2 > 0.015$ as the threshold for rearrangement (This threshold is set by the noise level in our D_{min}^2 calculation). Even for a relatively large strain amplitude, we still see a considerable fraction of particles which are not stroboscopically rearranging, and are reversible. Also note that the rearranging regions are scattered clusters of particles. The spatial correlation of D_{min}^2 for rearranging particles (red) is shown in Fig. 3c,d. For $\phi = 0.20$, the correlation length remains almost the same by increasing γ_0 , except for the largest amplitude case. However, for $\phi = 0.32$, the correlation length is highly dependent on the strain amplitude. As we move to a denser state, the thermal effects become negligible, and the dynamics is mostly governed by external driving. These correlation length measurements make clear that we have two distinct systems: One in which thermal energy is the dominant cause of rearrangements, and is relatively insensitive to shear; and another system in which the rearrangements are very sensitive to shear. Similar behaviour is observed in simulation by moving the system from shear dominated to thermal dominated regime [22].

Previous studies on a jammed athermal system, identified plastic reversible particles [11–13]. A plastic reversible particle undergoes a completely reversed rearrangement within a strain cycle, where the rearrangement path has hysteresis. In order to identify hysteresis, we define the strain at which a given particle starts to rearrange as γ^{on} , and the strain at which the particle stops rearranging as γ^{off} . For a hysteretic particle, $\gamma^{on} - \gamma^{off} \neq 0$.

We first study the stroboscopically reversible particles which undergo rearrangements within a given cycle. For this purpose, we measure D_{min}^2 between two peaks of a sinusoidal strain cycle, or the peak-to-peak D_{min}^2 . For the probed strain amplitudes, the fraction of particles undergoing peak-to-peak rearrangement is always larger than stroboscopic rearrangement (Fig. 4a,b). This indicates that a significant number of rearrangements are reversible. In Fig. 4c, we plot the fraction of particles which are stroboscopically reversible, while exhibit hysteresis in their rearrangement path. The fractions are obtained by considering all particles and all cycles excluding first 3 transient cycles. The data clearly indi-

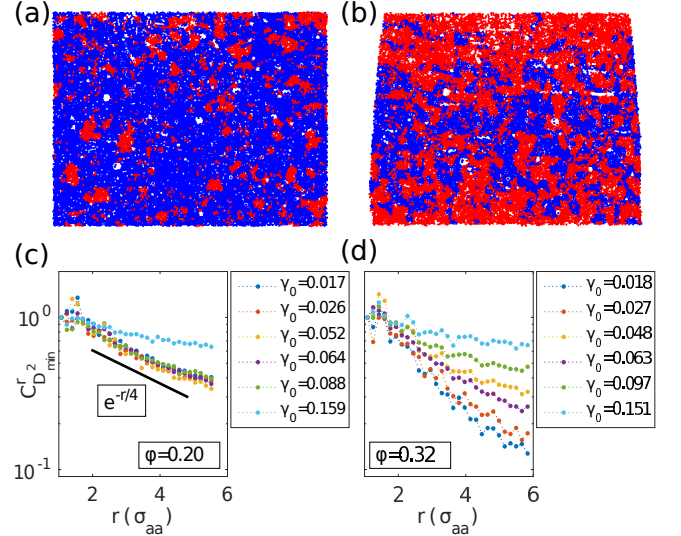


FIG. 3. Rearranging (Red), and nonrearranging (blue) particles for a) $\gamma_0 = 0.017$, and b) $\gamma_0 = 0.158$. Both (a) and (b) are plotted for cycle 15. c,d) Spatial correlation of D_{min}^2 for $\phi = 0.20$ and $\phi = 0.32$.

cate the existence of plastic reversible cycles in thermal systems, which was yet to be observed experimentally. We also note that the fraction of plastic reversible particles is considerably smaller for $\phi = 0.20$, compared to $\phi = 0.32$. Although irreversible particles are more frequent for $\phi = 0.20$, but the hysteresis of rearrangements for its reversible particles is significantly lower. Since the thermal fluctuations are stronger at lower packing fractions, the dynamics is closer to equilibrium, and hence, non-dissipative. By increasing the packing fraction, thermal fluctuations are hindered and the system regains athermal properties.

On the other hand, for a dense athermal system, once a particle enters into a reversible cycle, it remains reversible in the upcoming cycles [12]. In contrast, thermal noise allows the particles to escape reversible cycles with a certain probability (See Supplementary materials). In Fig. 5a, we show the transition probabilities (TP) between the reversible/irreversible states for various γ_0 . The TPs are measured by counting the number of particles transitioning from a particular state at cycle t , to another state at cycle $t+1$, and averaged over all cycles. We exclude 3 initial cycles to avoid transient states (TPs do not change significantly over non-transient cycles). For instance, $p[I^{t+1}|R^t]$ is the TP from a reversible to an irreversible cycle. The stability of reversible states can be quantified by $S_r = p[R^{t+1}|I^t] - p[I^{t+1}|R^t]$ (Fig. 5b). Both reversible cycles at low γ_0 , and irreversible cycles at high γ_0 are relatively more stable for $\phi = 0.32$ compared to $\phi = 0.20$. This is consistent with our earlier observation that thermal effects are hindered by increasing ϕ , and the system starts to behave athermally.

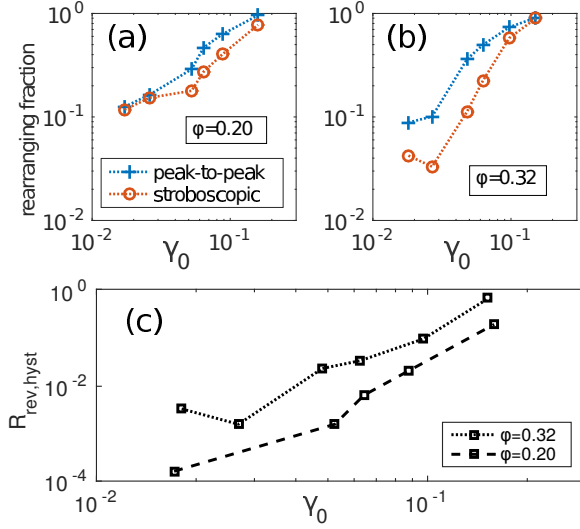


FIG. 4. a) Fraction of stroboscopic and peak-to-peak rearranging particles for $\phi = 0.20$, and b) $\phi = 0.32$. c) Fraction of hysteretic reversible particles ($R_{rev,hyst}$).

One can study the reversible-irreversible TPs within configurational energy landscape framework. Initially, a local energy minimum is occupied (Fig. 6a). Application of shear distorts and flattens the local minimum such that the system jumps to a nearby minimum state [23, 24]. For athermal particles, by reversing shear, the energy landscape resumes its original shape, and the system jumps back to the initial local minimum (reversible regime). This implies the existence of a metabasin in the energy landscape which confines the dynamics to a small region in configurational space [24–27]. By increasing the shear amplitude, the distortion of the energy landscape is large enough, such that the system escapes from the metabasin and the trajectories become irreversible. If, in addition to shear, the particles are also thermally activated, the system has a finite probability to escape the metabasin (Fig. 6b). As the thermal energy increases, the probability of escaping the metabasin, and hence irreversibility, also increases.

In conclusion, we described a cyclic shear experiment on a quasi-2D Brownian colloid. To our knowledge, this is the first experimental study that directly measures thermal fluctuations under shear for a large number of particles (2×10^4) and for relatively long times. Particle trajectories display a diffusive behavior consistent with unjammed, liquid-like state. Stroboscopic rearrangements are investigated for two values of packing fractions, $\phi = 0.20$, and $\phi = 0.32$. We find that the correlation length of rearrangements remains almost constant for the low packing fraction case, $\phi = 0.20$, while for $\phi = 0.32$ the correlation length is strongly dependent on strain amplitude. This indicates that for higher packing fractions thermal effects are hindered and shear is the dominant

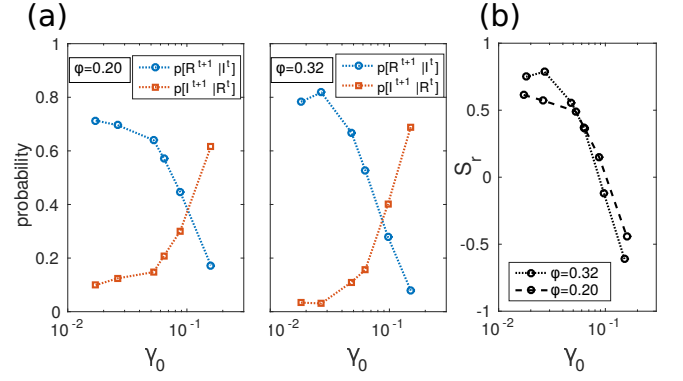


FIG. 5. Transition probabilities between reversibility states as a function of strain amplitude, γ_0 .

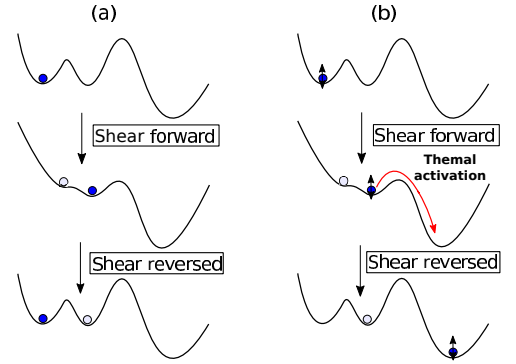


FIG. 6. Schematics of the state dynamics as a result of shear induced activation for a) athermal, and b) thermal systems.

driving mechanism for rearrangements. Further analysis of particle rearrangements showed that, similar to dense athermal systems, a fraction of particles undergo plastic reversible cycles, which decrease in number as the packing fraction is lowered. In other words, plastic reversibility is diminished as we move the system to thermal equilibration, here by lowering ϕ . We also observed that, for thermally activated systems, unlike jammed athermal systems, the particles escape from reversible states with a certain probability which depends both on packing fraction and strain amplitude. We find that for sufficiently small strain amplitudes, the reversible cycles are relatively more stable for higher packing fractions. This suggests that as the liquid is moved close to its glass transition point, the combination of thermal energy and shear is not sufficient to overcome the energy barrier and rearrange the particles towards equilibrium.

We would like to thank N. Keim, A. Yodh, and A. Liu for helpful discussions and suggestions, as well as Madhura Gurjar for the experimental setup design. This work was supported by NSF-Penn-MRSEC-DMR-1120901 and ACS-PRF-53948-ND9.

-
- [1] C. Royall, S. Williams, *Physics Reports* **560**, 1-75 (2015).
 - [2] L. Berthier, G. Biroli, *Rev. Mod. Phys.* **83**, 587 (2011).
 - [3] H.W. Sheng, W.K. Luo, F.M. Alamgir, J.M. Bai, E. Ma, *Nature* **439**, 419-425 (2006).
 - [4] T.K. Haxton and A.J. Liu *PRL* **99**, 195701 (2007).
 - [5] I.K. Ono, C.S. O'Hern, D.J. Durian, S.A. Langer, A.J. Liu, S.R. Nagel, *PRL* **89**, 095703 (2002).
 - [6] D. Chen, D. Semwogerere, J. Sato, V. Breedveld, E.R. Weeks, *Phys. Rev. E* **81**, 011403 (2010).
 - [7] V. Chikkadi, P. Schall, *Phys. Rev. E* **85**, 031402 (2012).
 - [8] E. Leutheusser, *Phys. Rev. A* **29**, 2765 (1984).
 - [9] L. Berthier, J.L. Barrat, *Phys. Rev. Lett.* **89**, 095702 (2002).
 - [10] R. Yamamoto, A. Onuki, *Phys. Rev. E* **58**, 3515 (1998).
 - [11] N.C. Keim and P.E. Arratia, *Soft Matter* **9**, 6222 (2013).
 - [12] N.C. Keim, P.E. Arratia, *PRL* **112**, 028302 (2014).
 - [13] N.C. Keim and P.E. Arratia, *Soft Matter* **11**, 1539 (2015).
 - [14] E.R. Weeks, D.A. Weitz, *PRL* **89**, 095704 (2002).
 - [15] M.T. Dang, D. Denisov, B. Struth, A. Zacccone, P. Schall, *Eur. Phys. J. E* **39**, 44 (2016).
 - [16] L. Berthier, G. Biroli, J.-P. Bouchaud, L. Cipelletti, D. El Masri, D. L'Hôte, F. Ladieu, M. Pierno, *Science* **310**, 1797 (2005).
 - [17] E. Weeks, D. Weitz, *Chemical Physics* **284**, 361 (2002).
 - [18] V. Prasad, D. Semwogerere, E.R. Weeks, *J. Phys.: Condens. Matter* **19**, 113102 (2007).
 - [19] E.R. Weeks, J.C. Crocker, A.C. Levitt, A. Schofield, D.A. Weitz, *Science* **287**, 627 (2000).
 - [20] trackpy: <http://dx.doi.org/10.5281/zenodo.34028>.
 - [21] M.L. Falk and J.S. Langer, *Phys. Rev. E* **57**, 7192 (1998).
 - [22] V. Chikkadi, S. Mandal, B. Nienhuis, D. Raabe, F. Varnik, P. Schall, *EPL* **100**, 56001 (2012).
 - [23] D.J. Lacks, *PRL* **87**, 225502 (2001).
 - [24] I. Regev, J. Weber, C. Reichhardt, K.A. Dahmen, T. Lookman, *Nat. Commun.* **6**, 9805 (2015).
 - [25] M.D. Ediger, P. Harrowell, *J. Chem. Phys.* **137**, 080901 (2012).
 - [26] V.J. Anderson, HNW. Lekkerkerker, *Nature* **416**, 811 (2002).
 - [27] R. Möbius, C. Heussinger, *Soft Matter* **10**, 4806 (2014).